Article

Metabolomic and Histological Response of *Passiflora cincinnata* Infected with *Cowpea aphid-borne mosaic virus* (CABMV) Reveals Changes in Asymptomatic and Symptomatic Phases

Paulo R. R. Mesquita, ✶*,a,b* Naira C. S. Barbosa,*c* Fábio N. dos Santos,*d*
Frederico M. Rodrigues,*a,b* Emanuel F. M. Abreu,*e* Kelly R. B. Leite,*c* Onildo N. Jesus,*f*
Andréia I. Tumelero,*f* Alessandra S. Schnadelbach*c* and Cristiane J. Barbosa*f*

*aCentro Tecnológico Agropecuário do Estado da Bahia (CETAB),
Avenida Milton Santos, 967, 40170-110 Salvador-BA, Brazil*

*bCentro Universitário Maria Milza, BR 101, Km 215,
44350-000 Governador Mangabeira-BA, Brazil*

*cInstituto de Biologia, Universidade Federal da Bahia, Rua Barão de Jeremoabo, 668,
40170-290 Salvador-BA, Brazil*

*dLaboratório ThoMSon de Espectrometria de Massas, Instituto de Química,
Universidade Estadual de Campinas, 13083-970 Campinas-SP, Brazil*

eEmbrapa Recursos Genéticos e Biotecnologia, 70770-917 Brasília-DF, Brazil

fEmbrapa Mandioca e Fruticultura, 44380-000 Cruz das Almas-BA, Brazil

Passion fruit woodiness disease, caused by the *Cowpea aphid-borne mosaic virus* (CABMV), is one of the leading phytosanitary challenges of passion fruit production. *Passiflora cincinnata* has been recognized for its potential in genetic improvement due to its highest resistance to CABMV and other phytopathogens. Metabolomic and histological alterations of *P. cincinnata* infected with CABMV were evaluated and searched for differential responses during the asymptomatic or symptomatic infection phases to correlate them with the mechanisms of metabolic defense. The metabolites of infected plants were analyzed by liquid chromatography-mass spectrometry. Based on the metabolomic profile, the times of infection were grouped into early or late infection phases. The metabolites related to CABMV infection were classified as alkaloids, saponins, phospholipids and acids. This study can assist agricultural institutions or farms in the early diagnosis and correct management of CABMV infection and contribute to the genetic improvement of the *Passiflora* genus against this disease.

Keywords: Passifloraceae, passion fruit woodiness disease, plant virus infection, agricultural pests, UHPLC-MS/MS

Introduction

The family Passifloraceae includes around 932 species and 36 genera[1] and has pantropical distribution.[2] The genus *Passiflora* is the most numerous among them, with approximately 560 species known as passion fruit,[3] most of which originate from Tropical America.[4] Brazil is one of the largest producers of yellow passion fruit (*Passiflora edulis* Sims), with an annual production of nearly 700,000 tons.[5]

In Brazil, the *Cowpea aphid-borne mosaic virus* (CABMV), of the family Potyviridae and genus *Potyvirus*, is the causative agent of passion fruit woodiness disease (PWD).[6] PWD is considered the most economically relevant factor limiting passion fruit production in the country, causing significant damage, such as reduced plant development, leaf mosaicism, blistering and distortion, and fruit woodiness.[7] Aphids are known to transmit the virus in a non-circulative and non-persistent manner.[8] Currently, there are no effective methods of control or eradication of the disease in commercial orchards, thus constituting another aggravating factor.[8,9]

Several wild *Passiflora* species have been identified as being tolerant to a variety of pests and diseases,[10-12] a fact that could render them ideal for genetic improvement programs involving interspecific hybridization. The species *P. cincinnata* Mast. is an alternative in PWD tolerance programs due to its high tolerance to CABMV.[10,12,13]

Passiflora cincinnata is an agronomically notable species because its fruit has a characteristic flavor desired by most consumers.[14] Moreover, it presents relevant agricultural characteristics, including significant levels of flavonoids and alkaloids,[15,16] which are important for pharmaceutical application, such as ethylhexyl methoxycinnamate and benzophenone-3, both used in the cosmetic industry.[17]

Histological changes in plants may occur as a cause or consequence of metabolic alterations due to virus infection. Anatomical changes can also be observed,[18-20] although there are only a few studies on such alterations resulting from CABMV infection in *Passiflora* species.[12]

One of the most effective plant responses to pathogen infection is the synthesis and accumulation of primary and secondary metabolites.[21,22] These substances are the end products of plant gene expression[23] and environmental factors, such as pathogen attack.[21,22] Pathogen-infected plants produce specific metabolites that play various roles in plant-pathogen interactions, including signal transduction, enzyme regulation, cell-to-cell signaling, and antimicrobial activity against pathogen attack.[24] These metabolites are accumulated in response to infection, working as plant defense mechanisms, and can constitute a genetic resistance indicator. Soybean plants infected by the oomycete *Phytophthora sojae* produce several sugars and secondary metabolites that are accumulated in resistant cultivars, though not in susceptible ones, hinting that these molecules may play a role in pathogen defense.[25]

Metabolomic approaches are able to detect minor changes in the metabolic profiles of plants in response to the attack of pathogens and differential metabolites throughout infection.[26] Metabolomic data can provide a broader view of the pathways involved in infection signaling and defense response to pathogen attack. Plants infected with viruses present modifications in their metabolic profile in response to interactions with the pathogen before histological alterations and the manifestation of symptoms.[27,28] The metabolomic approach can be used to detect many kinds of metabolites related to infection, such as molecules secreted by pathogens during infection[29] or amino acids and sugars, whose production is induced or mislocalized in the host to enhance the infection process. *B. cinerea*-infected strawberry plants exhibit distinct metabolomic profiles compared to healthy plants in the latent period, reflecting metabolic plant-

pathogen interactions.[30] Alkaloids comprise a class of natural bioactive compounds found in 20% of all vascular plants[31] that are well-known for their metabolic effects in mammals, e.g., caffeine, nicotine, morphine, strychnine, and cocaine, and have probably evolved as defense mechanisms against insect herbivory.[32] Alkaloids derived from quinolizidine, such as cytisine and sparteine, are efficient feeding deterrents against a number of herbivores.[33] *Solanum demissum* (nightshade potato), which contains the alkaloid demissine, is resistant to *Leptinotarsa decemlineata* (Colorado beetle) and *Empoasca fabae* (potato leafhopper).[34] Pyrrolizidine alkaloids are very potent antifeedants and extremely toxic to the aphid *Rhopalosiphum padi* and the milkweed bug *Oncopeltus fasciatus*.[31] Epicuticular wax is also composed of different types of compounds, including *n*-alkanes, primary alcohols, fatty acids, aldehydes, alcohols, diketones, and *n*-alkyl esters. However, its composition may be altered due to pathogen infection or damage caused by insects.[35] Viruses that rely on insect vectors are able to induce changes in epicuticular waxes, altering their composition and the reflective polarization properties of the infected host's leaves, thus facilitating their transmission by insects.[36]

Metabolites from several species of *Passiflora* have been identified in recent years due to their bioactive properties.[37] According to the study by Leal *et al.*,[38] *P. cincinnata* contains phenolic compounds and many other metabolites that can be a source of natural antioxidants of interest to the pharmaceutical industry, which have also been associated with plant resistance to pathogens.[39] Recent studies[40-43] involving the application of metabolomics have shown promise in understanding plant-pathogen interactions and plant pathology. However, there is a lack of studies regarding the metabolomic alterations of *P. cincinnata* in the PWD pathosystem that could help explain some resistance mechanisms to CABMV and contribute to assisting genetic improvement programs aiming at resistance to this pathogen.

The aim of the present study was to apply mass spectrometry-based metabolomics, associated with multivariate data analysis, to determine the metabolomic changes of *P. cincinnata* during infection by CABMV and investigate if there are associations between histological and metabolic alterations.

Experimental

Plant material

P. cincinnata seeds were obtained from the passion fruit germplasm bank at Embrapa Cassava and Fruits. They were planted in 16 cm-diameter pots containing a 1:1 mixture

of soil and vermiculite and subsequently irrigated once a day. Fourteen plants with three pairs of "true leaves" were maintained in a greenhouse at 25 ± 3 °C for biological analyses.

CABMV inoculation and biological trial

The biological trial was carried out in a greenhouse at Embrapa Cassava and Fruits, located in the city of Cruz das Almas, Bahia State, Brazil. The CABMV isolate of *P. edulis* from Cruz das Almas was propagated extensively in new healthy plants every two months in the greenhouse. Infection with CABMV was detected successively by reverse transcription polymerase chain reaction (RT-PCR), and the phytosanitary control of viral insect vectors, such as whiteflies and aphids, was conducted weekly. The isolate was used for biological purification using a previously described local lesion technique.[44] The inoculate solution was prepared using macerated leaf tissue at a ratio of 1 g of leaf tissue to 10 mL of 0.1 M sodium phosphate buffer solution (pH 7.0),[45] and the extract was applied mechanically on the leaf via basal leaves (with the exception of the cotyledons). A total of eight *P. cincinnata* plants (n = 8) were inoculated using a leaf sample exhibiting severe symptoms of PWD, while another six (n = 6) were inoculated with buffer and celite as a control. From the 6th until the 13th day post-inoculation (dpi), all samples were analyzed for systemic CABMV infection by RT-PCR, which enabled the amplification of genomic fragments corresponding to the cylindrical inclusion (CI) region of approximately 997 bp in infected plants. After 10 min of inoculation, the leaves were washed to remove excess celite.

Detection of the CABMV isolates

The leaves of the CABMV-infected plants underwent RT-PCR analysis (Thermo Scientific, Waltham, USA). Viral RNA was extracted from the samples according to the procedure described by Abreu *et al.*[46] and was used as a template for complementary deoxyribonucleic acid (cDNA) synthesis using Taq Platinum DNA polymerase (Thermo Scientific, Waltham, USA) and the following primer pair: CABMVF (5'-TKGTGTGRTAGAYTTTGGCTTKAAAGT-3') and CABMV2R (5'-GTCAYCCCMARRAGRGWRTGCAT-3'). The amplified 997 bp fragment corresponded to the CI (cylindrical inclusion) partial coding sequence. PCR amplification was performed with an initial heating step at 94 °C for 3 min, followed by 40 cycles of denaturation (94 °C for 1 min), annealing (50 °C for 1 min), and extension (68 °C for 4 min), and a final extension step (68 °C for 10 min). The PCR products of the CABMV isolates were purified using

the GenElute PCR Clean-Up Kit (Sigma-Aldrich, St. Louis, USA) and sequenced at Macrogen Inc. (Seoul, South Korea) using the primer pair set described above.

Sample preparation for metabolomic analysis

For the metabolomic analysis, the third pair of leaves from the base were removed from the healthy or inoculated plants with the CABMV isolate at 0, 3, 5, 8, 12, and 28 dpi. The leaves were removed before (T-1) and right after inoculation with either virus or buffer (T0). The *P. cincinnata* leaves were excised using sterilized scissors and were immediately macerated in liquid nitrogen to stop metabolism due to excision. Approximately 100 mg of the ground powder was extracted using 1 mL of methanol for 10 min at room temperature under vortex at 1,000 rpm (Multi Reax, Heidolph, Germany), followed by centrifugation at 12,000 × g for 5 min at 20 °C (Centrifuge 5418, Eppendorf, Hamburg, Germany). The supernatants were stored at –20 °C until further analysis. For the liquid chromatography-mass spectrometry (LC-MS) analysis, 50 μL of the concentrated extract was diluted in 950 μL of methanol in a vial before injection.

Metabolomic analysis

The extracts of infected or uninfected leaves were analyzed through a 1290 Infinity Liquid Chromatograph (ultra-high performance liquid chromatography (UHPLC)) coupled to an Agilent 6550 iFunnel quadrupole time-of-flight mass spectrometer (Q-TOF MS) (Agilent Technologies, Santa Clara, USA). Agilent Dual Jet Stream electrospray ionization technology (ESI, Agilent Technologies, Santa Clara, USA) was used as an ionization source in positive or negative ion mode. A Kinetex XB-C18 Core-Shell column (2.1 × 150 mm, 1.7 μm, 100 Å; Phenomenex Inc., Torrance, CA, USA) was maintained at a flow rate of 0.35 mL min^{-1} at 40 °C for the metabolite separation of 2 μL of extract using 0.1% aqueous formic acid as the aqueous phase and 0.1% formic acid in methanol as the organic phase. The chromatographic gradient of the organic phase was increased from 5 to 95% over 18 min and maintained for 7 min at 95%, returning to 5% in 8 min, which was equilibrated for 7 min. The extracts were kept in a freezer at –20 °C and, prior to analysis, they were placed in an autosampler maintained at a room temperature of approximately 21 °C. The quality control (QC) samples consisted of a pool of all the different inoculation times and controls and were analyzed at the beginning and end of each batch and after every ten injections.[26]

The ESI ionization source was used adopting the following conditions: drying gas temperature 250 °C;

drying gas flow rate 14.0 L min^{-1}; sheath gas temperature 250 °C; sheath gas flow rate 10.0 L min^{-1}; nebulizer gas 45 psig, and capillary voltage +3.5 or –3.5 kV for the positive or negative ions, respectively. The Q-TOF analyzer registered spectra in high-resolution mode (2 GHz) at a rate of 1.0 spectra s^{-1} within the *m/z* 100-1700 amu range. The skimmer voltage was adjusted to 65 V, octupole RF (radio frequency) at 750 V, fragmentor at 150 V, and nozzle voltage at 350 V. The reference mass ions (*m/z* 121.0509, 922.0098 in the positive and *m/z* 119.0363, 966.0007 in the negative) were orthogonally sprayed for accurate mass measurement. Mass tuning was performed using an Agilent tune mix (Santa Clara, USA) containing ions from 100 to 1600 Da. The spectra were recorded in full-scan mode along the entire mass range, as well as in auto-MS/MS mode for fixed energies of 30, 40, or 50 eV.[26]

LC-MS-based metabolomics data

LC-MS data processing was performed on the raw data, which was converted into mzData format using the MassHunter Qualitative Analysis software (Agilent Software B07.00, Santa Clara, CA, USA). The XCMS online platform[47] was used for feature detection, retention time correction, feature alignment, and univariate statistical analysis of the uploaded mzData files. An unpaired parametric *t*-test (Welch test) was used to identify significant features with a *p*-value threshold of 0.05 and a fold change threshold (highly significant features) of 1.5.[26] The MetaboAnalyst 3.0 platform[48] was used as an integrity check, missing value check, data filter, and in the statistical normalization analysis of features (*m/z*, retention times and intensities) for all samples of infected and noninfected leaves.

Sample preparation for histological analyses

Segments of the central vein region of the fifth leaf, from apex to base, were collected at 60 dpi.[11] Before gathering the samples, the symptoms of each leaf were analyzed. The fifth leaf from the apex to the base of each plant was deemed the sample for histological analyses. Samples from the healthy or infected plants were fixed in formaldehyde, acetic acid, and 70% ethanol, in the proportion of 1:1:18 (FAA$_{70}$) for 48 h and preserved in 70% ethanol, according to the method described by Johansen.[49] Subsequently, the leaf segments were dehydrated in an increasing ethylic series (85-100%) for 9 h, followed by slow infiltration in a historesin:ethanol solution, with 1:2 and 1:1 ratios, for 72 h each, and finally, in pure historesin, for a period of 7 days. The samples were then blocked and submitted to polymerization at room temperature for 48 h. Serial histological sections (5 μm) were obtained using a Leica RM 2155 rotary microtome (Leica, Nussloch, Germany).

Scanning electron and optical microscopy

In order to analyze the leaf epidermis by scanning electron microscopy, leaf segments of one infected and one healthy plant were dehydrated in an ethanol series, submitted to critical point drying, and coated with gold. The scanning electron images were obtained using the JEOL® JSM-6930LV microscope (JEOL, Akishima, Japan) of the Gonçalo Muniz Electron Microscopy Platform Research Center at the Oswaldo Cruz Foundation (FIOCRUZ-ME-CPqGM).

Sections for optical microscopy analyses were obtained from three infected and three healthy plants (control treatment). Paradermic sections of the leaf blades were cut manually with the help of a razor blade, then underwent clarification with 50% sodium hypochlorite,[50] were stained with 1% alcoholic safranin, and mounted on semi-permanent slides with 50% glycerin. Fragments of the leaves were also dehydrated in an ethanol series,[49] embedded in methacrylate, according to the manufacturer's instructions (Historesin, Leica, Nussloch, Germany), and transversely sectioned using a rotary microtome. The sections were stained with 0.05% toluidine blue[51] and mounted on permanent slides in Entellan® medium (Merck, Darmstadt, Germany). Photographic documentation was carried out under a Carl Zeiss® Axio Scope A1 light microscope (Carl Zeiss®, Jena, Germany). The reagents used were provided by Sigma-Aldrich (St. Louis, USA).

Statistical analysis

For the statistical analysis, the photographs were used to conduct quantitative assessments to measure tissue thickness in the cross-sections of the leaf blade: thickness of the adaxial (Tad) and abaxial epidermis (Tab); thickness of the palisade (TPP) and spongy parenchyma (TSP), and total leaf thickness (TL) using the AxioVision® image program.[52] For each feature, 10 cuts of each leaf (30 units in total) were used. Stomatal counting was performed on the abaxial surface of the leaf blade to obtain the stomatal density *per* mm^2 using the ANATI QUANTI program.[53] Counting was carried out in 10 distinct regions of each of the 30 healthy and 30 infected leaves. The quantitative analysis of the histological data was based on the averages of the infected plants in relation to the healthy ones and was obtained using Student's *t*-test on the R program (R Core Team 2013).[54]

Results

CABMV inoculation and biological trial

The CABMV isolates from *P. edulis* was extensively propagated in new healthy plants every two months in a greenhouse. CABMV infection was detected successively by RT-PCR, and the phytosanitary control of viral insect vectors, such as whiteflies and aphids, was carried out weekly. A total of eight *P. cincinnata* plants (n = 8) were inoculated using a leaf sample with severe symptoms of PWD, while another six (n = 6) were inoculated with buffer as a plant control. From the 6th until the 13th dpi, all samples were diagnosed to assess for systemic infection of CABMV by RT-PCR, which enabled the amplification of genomic fragments corresponding to the cylindrical inclusion (CI) region of approximately 997 bp in infected plants (Figure 1a). This analysis was carried out from the sixth dpi on due to the variation in the detection of this virus in lesser times. The observed results could be associated with the time of establishment of systemic CABMV infection in *P. cincinnata*. Nevertheless, after 15 dpi, leaf mosaic symptoms were observed in all the inoculated *P. cincinnata* (Figure 1c).

Effect of mechanical inoculation on metabolomic profiles

In order to assess the effects of mechanical inoculation on the metabolomic profile of the plants, it was analyzed leaves without mechanical inoculation (T-1), leaves freshly inoculated with buffer (T0-CN), and leaves freshly infected with CABMV virus (T0-INOC) for analysis by LC-MS. The partial least squares-discriminant analysis (PLS-DA) scoring plot (Figure 2a) showed that the samples without mechanical inoculation (T-1) were grouped in distinct quadrants those mechanically inoculated (T0-CN or T0-INOC). Therefore, the mechanical inoculation procedure generated significant changes in the plants' metabolomic profiles. Furthermore, there were also metabolomic differences between the infected and control samples mechanically inoculated, given that they were separated into two clusters in the same quadrants of component 1. The variable importance in projection (VIP) scores showed a high abundance of highest scored metabolites for the infected samples mechanically inoculated (T0-INOC). Medium abundance of the highest scored metabolites for samples mechanically treated with buffer (T0-CN), and low abundance of the highest scored metabolites for samples without inoculation, confirming also the effect of infection on the metabolite changes (Figure 2b).

Effect of the CABMV virus infection on metabolomic profiles

We also investigate the effect of the CABMV virus infection on metabolomic profiles comparing infected samples at (T-1), (T0), (T3), (T5), (T8), (T12), (T20), and (T28) days *versus* buffer inoculated samples in the same times. Untargeted metabolomics revealed that, regardless of the post-inoculation time, there was clear discrimination between infected and control samples in two clusters (Figure 3). Therefore, from this point on, we show only the infected samples in order to highlight the differences
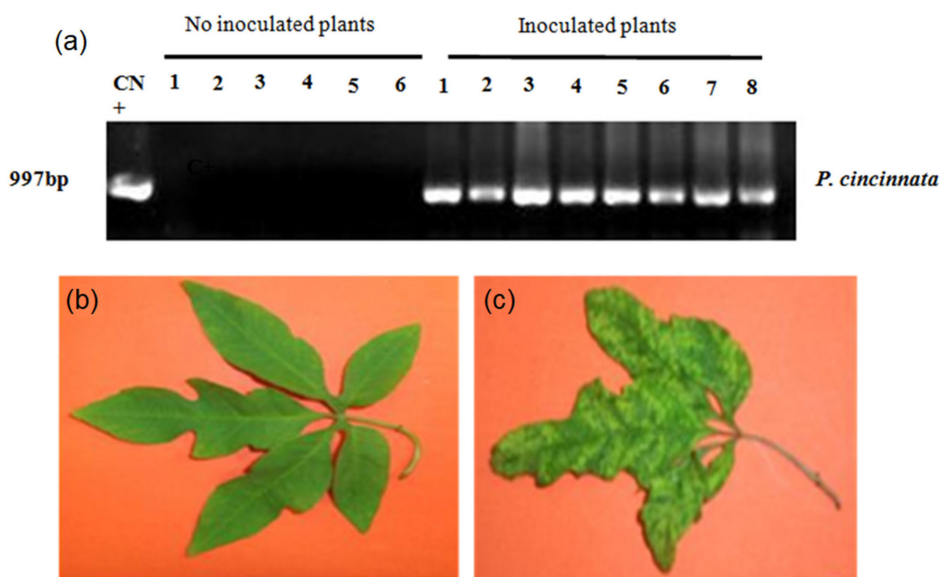
Figure 1. RT-PCR (997 base pair (pb)) of the *P. cincinnata* plants inoculated with CABMV. (a) Detection of the CABMV cylindrical inclusion region: infected *P. edulis*, used as a positive control (CN+); six samples of non-inoculated *P. cincinnata*, used as negative controls (CN–); eight samples of *P. cincinnata* collected at 6 or 13 dpi; (b) leaf of non-inoculated *P. cincinnata*, used as a control; (c) leaf of infected *P. cincinnata* with symptoms.
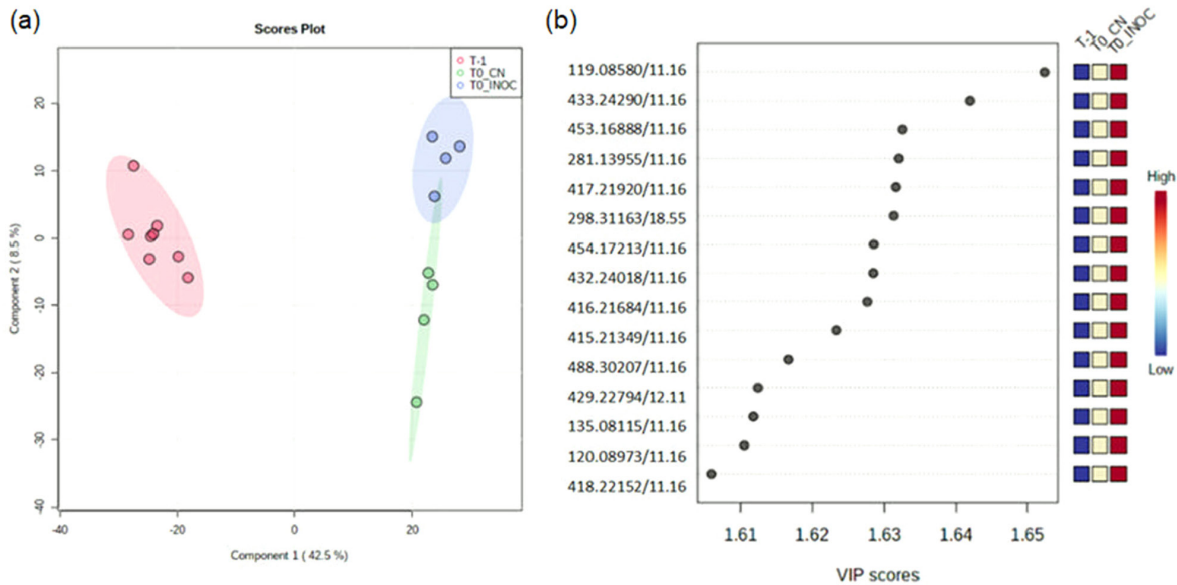
Figure 2. (a) PLS-DA scoring plots for the (T-1) and (T0) post-infection time points obtained from the LC-MS analysis in positive ion mode ESI(+); (b) VIP score-plot from the PLS-DA multivariate analysis. To the left of the VIP score-plot, the number indicates the exact mass/retention time; e.g., the code 119.0858/11 stands for m/z 119.0858 detected in positive mode and the retention time (11) of the feature. To the right of the VIP score-plot, the color grade varies from blue (low abundance) to red (high abundance). T-1: leaves removed before inoculation with either virus or buffer; T0: leaves removed right after inoculation with either virus (_INOC) or buffer (_CN).
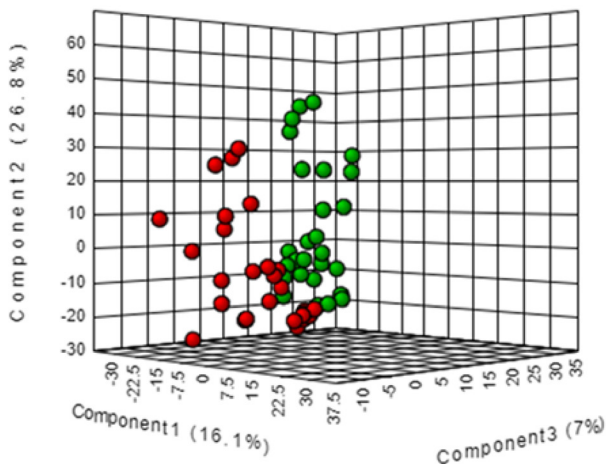
Figure 3. 3D PLS-DA scoring plots for the infected (red) and uninfected (green) plants analyzed by LC-MS in positive ion mode ESI(+) at (T-1), (T0), (T3), (T5), (T8), (T12), (T20), and (T28) days.

related to infection progression during asymptomatic and symptomatic phases.

In the PLS-DA scoring plots of the seven post-infection times and the control in T0 (Figure 4a), it can be noted that four different clusters were formed, corresponding to the without samples ((T-1), cluster I), buffer inoculated samples as positive control and freshly infected plants ((T0), cluster II), the early infection group ((T3), (T5), and (T8), cluster III), and the late infection times ((T12), (T20), and (T28), cluster IV). In addition to the alterations observed at the beginning of inoculation which the samples grouped in the samples quadrants ((T-1), (T0-CN) and

(T0-INOC)) were separated into clusters, a gradual change in the metabolic profile of the infected samples was verified in two phases, deemed as early ((T3), (T5), and (T8)) and late ((T12), (T20), and (T28)) infection phase. Depending on the metabolite the abundance increased or decreased into the early or late infection phase.

The VIP score-plot (Figure 4b) shows that the annotated ions m/z 793.5680 and 198.1856 increased in abundance during the progression of infection, whereas the abundance of the ions m/z 288.1967, 376.3515, and 404.3878 decreased.

The detected ions that exhibited significant changes due to the time of infection are shown in Figure 5. Some ions (m/z 198.18564, 207.13887, and 335.31489) displayed an increment in relative abundance between 0 and 28 days of infection (Figures 5a-5c). Meanwhile, others (m/z 288.19670, 336.31305, and 619.31195) presented a reduction in relative abundance during the same period (Figures 5d-5f). The discriminant molecular features were annotated using MS and MS/MS spectra in the MS-Finder database (Table 1).

Scanning electron and optical microscopy

By means of scanning electron microscopy, it was possible to observe the presence of epicuticular wax with a crystalloid aspect in both epidermal faces of the adaxial and abaxial surfaces of the *P. cincinnata* leaves. This outcome was seen in both healthy (non-inoculated) and infected
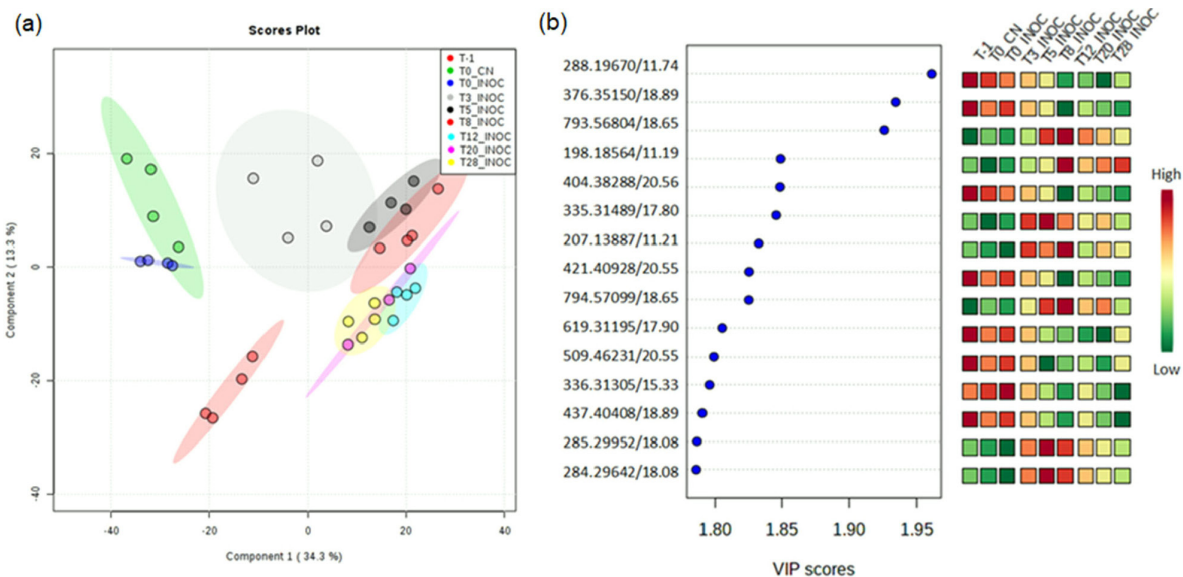
Figure 4. (a) PLS-DA scoring plots for infected or buffer inoculated samples analyzed by LC-MS in positive ion mode ESI(+) at (T-1), (T0), (T3), (T5), (T8), (T12), (T20), and (T28) days; (b) VIP score-plot derived from the PLS-DA multivariate analysis obtained from LC-MS in positive ion mode ESI(+). To the left of the VIP score-plot, the number indicates the exact mass/retention time; e.g., the code 288.19671/11.74 stands for *m/z* 288.1867 detected in positive mode and the retention time (11.74) of the feature. To the right of the VIP score-plot, the color grade varies from green (low abundance) to red (high abundance). T-1: leaves removed without inoculation with either virus or buffer; T0: leaves removed freshly after inoculation with either virus (_INOC) or buffer (_CN).
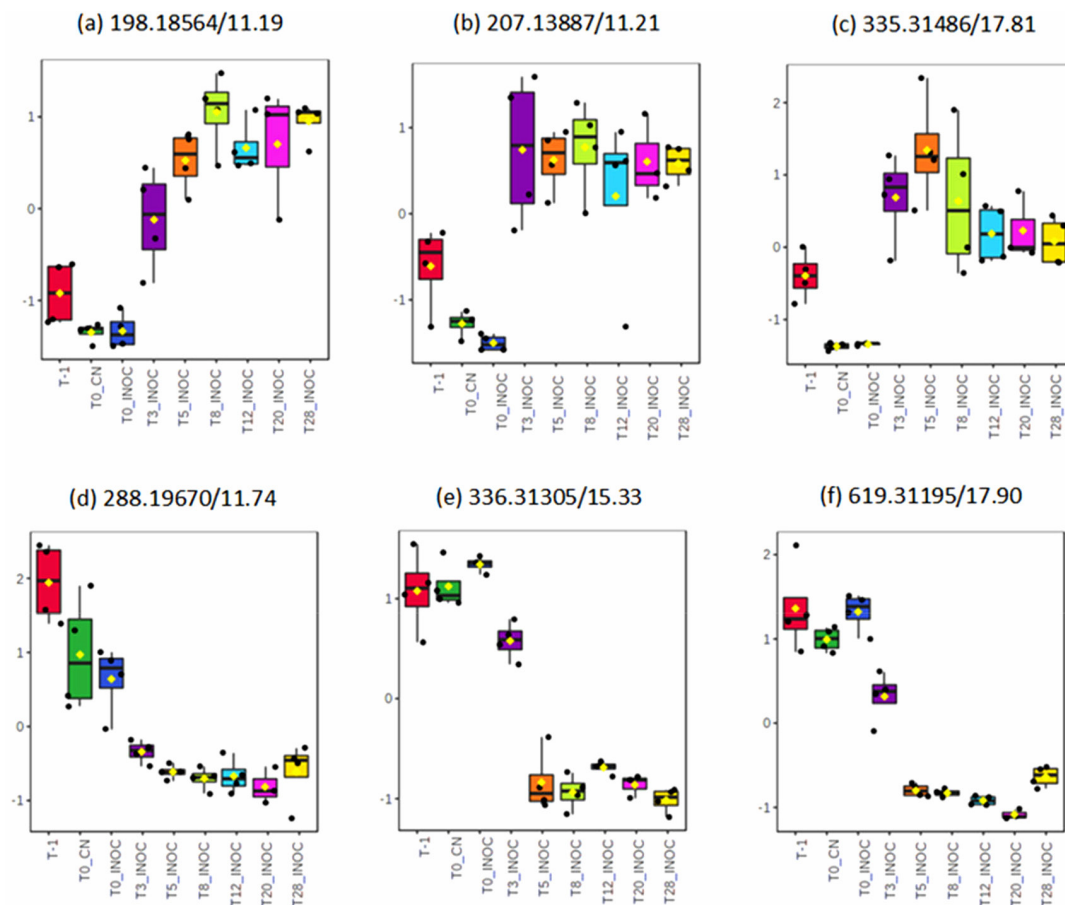
Figure 5. Box-plots from the s-plot of the molecular features of the discriminated metabolites of infection of infected and uninfected plants analyzed by LC-MS in positive ion mode ESI(+) at (T-1), (T0), (T3), (T5), (T8), (T12), (T20), and (T28) days (identified in Table 1): (a) *m/z* 198.18564; (b) *m/z* 207.13887; (c) *m/z* 335.31486; (d) *m/z* 288.19670; (e) *m/z* 336.31305; (f) *m/z* 619.31195. T-1: leaves removed before inoculation with either virus or buffer; T0: leaves removed right after inoculation with either virus (_INOC) or buffer (_CN).

Table 1. Major metabolites identified in the VIP score-plots related to *Cowpea aphid-borne mosaic virus* infection annotated using LC-MS/MS data. Annotation level: identified metabolites (level 1), putatively annotated compounds (level 2), putatively characterized compound classes (level 3), and unknown compounds (level 4)

Metabolite	t_R^a / min	Molecular formula	Annotation level	*m/z* Theor.[b]	*m/z* Detected	AME[c] / ppm	Adduct
Isolobinine	11.74	$C_{18}H_{25}NO_2$	2	288.19581	288.19670	3.1	$[M + H]^+$
Unknown	18.89		4		376.35150	–	
PA(22:2(13Z,16Z)/19:0)	18.65	$C_{44}H_{83}O_8P$	2	793.57178	793.56804	4.7	$[M + Na]^+$
Homodihydrojasmone	11.19	$C_{12}H_{20}O$	2	198.18524	198.18564	2.0	$[M + NH_4]^+$
Unknown	13.15		4		404.38288	–	
Ormosanine	17.81	$C_{20}H_{35}N_3$	2	335.31692	335.31486	6.0	$[M + NH_4]^+$
Plastoquinol-1	11.21	$C_{13}H_{18}O_2$	2	207.13796	207.13887	4.4	$[M + H]^+$
Unknown	20.55		4		421.40928	–	
Glycerophospholipid (PC)	18.65	$C_{45}H_{80}NO_8P$	3	794.56943	794.57099	2.0	$[M + H]^+$
Virgaureasaponin I	17.90	$C_{59}H_{96}O_{27}$	2	619.31423	619.31195	3.7	$[M + 2H]^{2+}$
Unknown	20.55		4		509.46231	–	
Juliflorine	15.33	$C_{40}H_{75}N_3O_2$	2	336.31300	336.31305	1	$[M + CAN + 2H]^{2+}$
Unknown	18.89		4		437.40408	–	
Glycerophospholipid (PA)	18.08	$C_{47}H_{85}O_8P$	3	285.29940	285.29952	2	$[M + H + 2Na]^{3+}$
Stearamide	18.09	$C_{18}H_{37}NO$	2	284.29479	284.29642	5.7	$[M + H]^+$

[a]t_R: retention time; [b]Theor: theoretical *m/z*; [c]AME: atomic mass evaluation.

plants, as shown in Figure S1 (Supplementary Information (SI) section).

In the paradermic and cross-sections of both sides of the leaf blades, stomata were observed only on the abaxial face, thus classifying the leaves as hypostomatic. In frontal view, polygonal epidermal cells of straight anticlinal to slightly winding walls were identified on the adaxial face (Figure S2a, SI section), while on the abaxial face, they exhibited a more tortuous outline. However, no differences were observed in the format of the cells when comparing the infected plants with the healthy ones (Figure S2a). In addition, two sets of circular bundles were found near the median region of the central vein, one larger and the other smaller, the latter turned towards the adaxial face. *P. cincinnata* did not present differences in cross-sections comparing infected and healthy plants (Figure S2b). Also, no changes in the vascular system were observed (Figure S2c).

According to the quantitative analyses results, *P. cincinnata* showed no anatomical differences due to the presence of CABMV, only regarding adaxial epidermis thickness (Tad) (Table S1, SI section).

Discussion

In the present study, we investigated the changes in metabolic and ultrastructural characteristics resulting from infection for a better understanding of *P. cincinnata*

defense against CABMV. A primary challenge in pathogen-host studies is finding true metabolic alterations related to virus infection, despite natural metabolic development, mechanical inoculation, or excision. The excision effect here was controlled by stopping metabolism via immersion in liquid nitrogen. Also, natural metabolic development was monitored through control samples in all infection times. Firstly, we evaluated if mechanical inoculation had any influence on metabolic alterations through buffer inoculation in contrast to without inoculated samples. The mechanical inoculation of buffer caused metabolic alterations without inoculated samples. Furthermore, virus inoculated samples showed metabolomic changes to buffer inoculated. Therefore, we adopted buffer inoculated samples to each infection time to correct such deviation. Interestingly, we noted that pathogen infection exhibited a greater effect on the increase in metabolite abundance than mechanical inoculation with buffer alone (Figure 1). In fact, the VIP scores showed that the highest scored metabolites were more abundant in the pathogen-inoculated samples when compared to the samples buffer inoculated.

Based on the results, we conducted mass spectrometry-based metabolomics to identify metabolites differentially accumulated in *P. cincinnata* after different times of infection with CABMV. Two separate clusters related to the buffer inoculated and infected plants demonstrated a specific metabolic response to CABMV infection. A gradual change in the metabolic profile of the infected

plants was observed, which can be attributed to the two phases of infection: early (at 3, 5, and 8 dpi) and late (at 12, 20, and 28 dpi); these two periods were correlated to asymptomatic and symptomatic phases of infection, respectively. The detection of alterations in the metabolic profile at an early stage of infection, even symptoms, is the best way to early diagnose CABMV disease in *P. cincinnata* plants. We emphasize that similar approaches involving the metabolic profile of plants have been used in other studies, e.g., to compare the phytochemical profile of different cinnamon species;[55] in the detection of metabolic differences between healthy and Huanglongbing (HLB)-affected Newhall navel oranges[56] and to find biomarkers that can distinguish different species of Cactaceae, besides to identifying secondary metabolites that confer resistance to *D. opuntiae*.[57]

In the late phase of infection, a significant change was observed in the *P. cincinnata* metabolomic profile associated with leaf symptoms. These results corroborate those reported by Gonçalves *et al.*,[11] who evaluated the symptom progression caused by CABMV in different *Passiflora* species. In their study, mean severity increased gradually in the interval from 20 to 55 dpi. According to their findings, the authors classified *P. cincinnata* in the group of species resistant to CABMV, a group that presented a later progression of symptoms of the disease.

Table 1 shows the main annotated metabolites in the *P. cincinnata* clusters in the early and late stages of infection. Isolobinine (annotated from ion *m/z* 288.19670) was more abundant in the uninfected plants, with decreased levels in the plants inoculated with the pathogen or buffer (Figure 5d). This compound can be considered an unspecific metabolite, and its loss during mechanical inoculation might have occurred through oxidation or some other process. It may also play a role in pathogen defense since its abundance was greater in the buffer-inoculated plants than the infected ones. This metabolite is a piperidine-type alkaloid that has been shown to present leishmanicidal,[58] antimalarial,[59] and schistosomicidal activity.[60]

The abundance of ormosanine (*m/z* 335.31486) was more significant in the early infection phase than in late infection, indicating that this metabolite may act in signaling or primary defense response (Figure 5c). Ormosanine is a pentacyclic alkaloid that has been previously shown[61,62] to exhibit analgesic and antimalarial behavior. Juliflorine (*m/z* 336.31305), on the other hand, displayed greater abundance in the uninfected plants, decreasing in concentration upon inoculation until (T3) dpi. However, a strong reduction in abundance occurred after (T5) dpi and in the late infection phase, suggesting that the metabolite is probably consumed during the defense

to pathogen attack (Figure 5e). This piperidinium alkaloid has been isolated from the leaves of *Prosopis juliflora*[63] and has demonstrated inhibitory potential against cholinesterase enzymes[64] and antileishmanial[65] and antifungal activity against *Aspergillus* species.[66]

Meanwhile, the abundance of homo-dihydrojasmone (annotated from ion *m/z* 198.18564) increased from early to late infection, possibly indicating that the metabolite is involved in a process activated in response to attack, since it showed activity throughout all phases of infection (Figure 5a). This cyclic ketone has compounds that have been reported[67] to be plasmin serine protease inhibitors. Dihydrojasmone has also been described[68] as acting in the natural mechanisms of plant defense, such as plant-aphid interactions.

Plastoquinol-1 (*m/z* 207.13887), in turn, was most abundant at (T3) dpi, decreasing in early infection and becoming constant during late infection (Figure 5b), evidencing its potential role in the signaling of infection and primary defense. This metabolite is a prenylhydroquinone that acts in the photosystem II of oxygenic photosynthetic organisms and is present in the plant's chloroplasts.[69] These organelles are involved in the basal and systemic antipathogenic defense response of plants,[70] and, therefore, they need to have such defense suppressed by the invading pathogen to generate a consequent metabolic alteration. In *Solanum nigrum* plants treated with the pathogen *Phytophthora infestans*, an increase in reactive oxygen species (ROS) production was observed, accompanied by a significant increment in plastoquinone (PQ) levels.[71] One hypothesis is that PQ may be associated with specific mechanisms that maintain a tightly controlled balance between the accumulation of ROS and antioxidant activity, that determines the full expression of effective defense.[72]

Virgaureasaponin I (*m/z* 619.31195) was highly abundant in the uninfected plants, decreasing after (T3) dpi; the largest drop in abundance was observed after (T5) dpi, as well as in the late infection phase. This triterpenoid saponin is consumed in the defense response of plants to pathogen attack (Figure 5f), having been described[73] to present activity against *Candida albicans* yeast-hyphal. In plants, saponins are also involved in plant defense against microbial or pest attacks,[74] and have been shown to exert insecticidal,[75] antiviral,[76] and molluscicidal activity,[77] as well as allelopathic action towards other plant species.[78]

The glycerophospholipid related to *m/z* 285.29940 was more abundant during early infection than in the late infection phase (Figure 4), indicating that it may act in signaling or primary defense response. Glycerophospholipids are polar phospholipids present in biological membranes. Some studies[79] evaluating plants infected with the brome mosaic

virus (BMV) have shown that there is a significant increase in phospholipid phosphatidylcholine content in yeast and barley cells. Like phospholipids, stearamide (annotated from *m/z* 284.29642) exhibited a similar tendency, presenting a higher abundance in the early infection phase than in late infection (Figure 4). Stearamide is a fatty acid amine that has been reported[80] to show antibacterial activity, in addition to being a potential psoriasis vulgaris biomarker in human plasma[81] and involved in metabolic changes in golden retriever muscular dystrophy.[82]

The results obtained herein regarding *P. cincinnata* leaf surface scanning electron microscopy revealed the presence of crystalloid epicuticular wax in both healthy and infected plants. This is probably a specific genetic anatomical feature of this and other wild *Passiflora* species.[83] Epicuticular wax comprises an active interface between plants and the environment, constituting a defense mechanism to abiotic and biotic stress. Thus, it protects the plant from the action of insects and infection by pathogens, including fungi, bacteria, and viruses.[35] Some studies have correlated epicuticular wax with tolerance to aphids in several species, such as cabbage (*Brassica oleracea* var. *acephala*),[84-86] raspberry (*Rubus ideaus*),[87] and pea (*Pisum sativum*).[88] This wax has been associated with the prevention of cotton leaf curl virus (CLCuV) transmission by the whitefly in white cotton (*Gossypium arboreum*), playing a role as a physical barrier to vector attack.[89] These studies suggest that the epicuticular wax observed in *P. cincinnata* may also be related to field resistance to CABMV and other pathogens observed in this species[4,12] since it may influence the process of acquiring and transmitting the virus by vectors and, thus, affect transmission efficiency.

According to the histological results, infection by CABMV in *P. cincinnata* apparently did not cause substantial damage to the structural organization of leaf tissue and cells since there was no significant difference in the shape of the cells of infected plants compared to healthy ones. The reduction in cell wall sinuosity can be attributed to the plant's adaptive characteristics against excessive water loss.[90,91] Moreover, cross-sectional alterations were not observed, nor in the vascular system of the infected or healthy plants. Only changes in the thickness of the adaxial epidermis (Tad) were noted in the histological experiments. Similar results were also described in the study[12] in which the authors assessed the resistance of several wild *Passiflora* species to CABMV. According to the authors, *P. cincinnata* was classified as resistant to CABMV since it exhibited mild mosaicism and did not present significant histological changes resulting from virus inoculation. Segments of the central vein region of the fifth leaf from the apex to the base were standardized as the sample of choice to

evaluate plants at 60 dpi since this method was considered sufficient to note possible histological changes resulting from CABMV infection.[11]

The present results obtained from the histological evaluation of CABMV-infected plants demonstrated that infection was not able to promote major changes in the leaf tissue of infected plants, except the reduced thickness of the upper surface, corroborating studies[10,12,13,92] that state that this species is resistant to CABMV. Despite the absence of structural alterations, the metabolite abundances identified herein, not yet described in infected *Passiflora* plants, reinforce the evidence of the production of metabolites in response to viral infection. These metabolic changes associated with crystalloid wax deposition on the leaf surface seem to be able to delay or inhibit the effects of viral infection, a fact that could explain the absence of histological differences between infected and healthy plants, as well as contribute to the resistance against CABMV.

Interspecific hybridization is one of the most used approaches in the genetic improvement of passion fruit,[93] aiming at transferring the resistance found in wild species to susceptible commercial species, such as *P. edulis*.[13] Thus, the anatomical and metabolomic characteristics observed in the wild species of *Passiflora*, described as resistant to CABMV, can constitute anatomical and biochemical markers for the selection of hybrids resistant to this virus.

Conclusions

This pioneering study investigated the plant-pathogen interactions related to CABMV disease in *Passiflora* species. We concluded that metabolomic changes caused by CABMV infection began in the asymptomatic phase by 8 dpi without apparent histological alterations. Then, metabolomic changes followed before symptoms that may appeared very late. The infection times were grouped into two clusters related to early or late stages of infection. The metabolites of the highest scored that were associated with infection phases were primarily alkaloids, saponins, and phospholipids. Plastoquinol-1, juliflorine, and ormosanine were more abundant in the early infection phase, whereas virgaureasaponin I was more abundant in the late infection phase. Homo-dihydrojasmone increased throughout the two stages. Our metabolomic approach comprises a tool for the early detection of CABMV infection into an asymptomatic phase that could be used to help farmers in the CABMV control.

Supplementary Information

Supplementary data are available free of charge at http://jbcs.sbq.org.br as PDF file.

Acknowledgments

Author Contributions

P. R. R. M., F. N. S., F. M. R., E. F. M. A., O. N. J. and C. J. B. designed the experiments. Material preparation, sample analysis, and data collection were conducted by P. R. R. M., N. C. S. B., F. N. S., A. I. T. and K. R. B. L. Data analysis was performed by P. R. R. M., F. N. S., F. M. R., E. F. M. A. and C. J. B. The first draft of the manuscript was written by P. R. R. M. and all authors contributed to the final version of the manuscript. A. S. S. supervised the project.

References

1. The Plant List, http://www.theplantlist.org/1.1/browse/A/Passifloraceae, accessed in May 2022.

2. Souza, V. C.; Lorenzi, H.; *Botânica Sistemática: Guia Ilustrado para Identificação das Famílias de Fanerógamas Nativas e Exóticas no Brasil*, baseado em APG III, 3rd ed.; Instituto Plantarum: Nova Odessa, Brazil, 2012.

3. Krosnick, S. E.; Porter-Utley, K. E.; Macdougal, J. M.; Jørgensen, P. M.; Mcdade, L. A.; *Syst. Bot.* **2013**, *38*, 692. [Crossref]

4. Oliveira, J. C.; Ruggiero, C. In *Maracujá: Germoplasma e Melhoramento Genético*; Faleiro, F. G.; Junqueira, N. T. V.; Braga, M. F., eds.; Embrapa Cerrados: Planaltina, Brazil, 2005, p. 143.

5. Instituto Brasileiro de Geografia e Estatística (IBGE), Produção Agrícola Municipal, https://sidra.ibge.gov.br/tabela/5457, accessed in May 2022.

6. Nascimento, A. V. S.; Santana, E. M.; Braz, A. S. K.; Alfenas, P. F.; Ribeiro, G. P.; Andrade, G. P.; Carvalho, M. G.; Zerbini, F. M.; *Arch. Virol.* **2006**, *151*, 1797. [Crossref]

7. Barbosa, C. J.; Santos Filho, H. P. In *Maracujá: do Cultivo à Comercialização*; Junghans, T. G.; Jesus, O. N., eds.; Embrapa: Brasília, Distrito Federal, Brazil, 2017, p. 281.

8. Cerqueira-Silva, C. B. M.; Santos, E. S. L.; Jesus, O. N.; Mori, G. M.; Corrêa, R. X.; Souza, A. P.; *Int. J. Mol. Sci.* **2014**, *15*, 22933. [Crossref]

9. Fischer, I. H.; Rezende, J. A. M.; *Pest Technology* **2008**, *2*, 1.

10. Junqueira, N. T. V.; Braga, M. F.; Faleiro, F. G.; Peixoto, J. R.; Bernacci, L. C. In *Maracujá: Germoplasma e Melhoramento Genético*; Faleiro, F. G.; Junqueira, N. T. V.; Braga, M. F., eds.; Embrapa Cerrados: Planaltina, Brazil, 2005, p. 81.

11. Gonçalves, Z. S.; Jesus, O. N.; Cerqueira-Silva, C. B. M.; Diniz, R. P.; Soares, T. L.; Oliveira, E. J.; *Biosci. J.* **2017**, *33*, 1441. [Crossref]

12. Gonçalves, Z. S.; Lima, L. K. S.; Soares, T. L.; Abreu, E. F. M.; Barbosa, C. J.; Cerqueira-Silva, C. B. M.; Jesus, O. N.; Oliveira, E. J.; *Sci. Hort.* **2018**, *231*, 166. [Crossref]

13. Oliveira, E. U.; Soares, T. L.; Barbosa, C. J.; Santos Filho, H. P.; Jesus, O. N.; *Rev. Bras. Frutic.* **2013**, *35*, 485. [Crossref]

14. Araújo, F. P.; Silva, N.; Queiroz, M. A.; *Rev. Bras. Frutic.* **2008**, *30*, 723. [Crossref]

15. Tsuchiya, H.; Shimizu, H.; Iinuma, M.; *Chem. Pharm. Bull.* **1999**, *47*, 440. [Crossref]

16. Gonulalan, E. M.; Nemutlu, E.; Bayazeid, O.; Koçak, E.; Yalçin, F. N.; Demirezer, L. O.; *Phytomedicine* **2020**, *74*, 152920. [Crossref]

17. Velasco, M. V. R.; Fsarruf, F. D.; Salgado-Santos, I. M. N.; Haroutiounian-Filho, C. A.; Kaneko, T. M.; Baby, A. R.; *Int. J. Pharm.* **2008**, *363*, 50. [Crossref]

18. Takimoto, J. K.; Voltan, R. B. Q.; Dias, J. A. C. S.; Cia, E.; *Bragantia* **2009**, *68*, 109. [Crossref]

19. Marques, J. P. R.; Kitajima, E. W.; Astua, J. F.; Glória, B. A.; *An. Acad. Bras. Cienc.* **2010**, *82*, 501. [Crossref]

20. Khalil, R. R.; Bassiouny, F. M.; El-Dougdoug, K. A.; Abo-Elmaty, S.; Yousef, M. S.; *Int. J. Agric. Technol.* **2014**, *10*, 1213.

21. Fiehn, O.; Kopka, J.; Dörmann, P.; Altman, T.; Trethewey, R.; Willmitzer, L.; *Nat. Biotechnol.* **2000**, *18*, 1157. [Crossref]

22. Fiehn, O.; *Plant Mol. Biol.* **2002**, *48*, 155.

23. Mesquita, P. R. R.; Nunes, E. C.; dos Santos, F. N.; Bastos, L. P.; Costa, M. A. P. C.; Rodrigues, F. M.; de Andrade, J. B.; *Microchem. J.* **2017**, *130*, 79. [Crossref]

24. Vinayavekhin, N.; Saghatelian, A.; *Curr. Protoc. Mol. Biol.* **2010**, *90*, 30.1.1. [Crossref]

25. Zhu, L.; Zhou, Y.; Li, X.; Zhao, J.; Guo, N.; Xing, H.; *Front. Plant Sci.* **2018**, *9*, 1530. [Crossref]

26. Garcia, P. G.; dos Santos, F. N.; Zanotta, S.; Eberlin, M. N.; Carazzone, C.; *Molecules* **2018**, *23*, 3330. [Crossref]

27. Bazzini, A. A.; Manacorda, C. A.; Tohge, T.; Conti, G.; Rodriguez, M. C.; Nunes-Nesi, A.; Villanueva, S.; Fernie, A. R.; Carrari, F.; Asurmendi, S.; *PLoS One* **2011**, *6*, e28466. [Crossref]

28. Sade, D.; Shriki, O.; Cuadros-Inostroza, A.; Tohge, T.; Semel, Y.; Haviv, Y.; Willmitzer, L.; Fernie, A. R.; Czosnek, H.; Brotman, Y.; *Metabolomics* **2015**, *11*, 81. [Crossref]

29. Tsuge, T.; Harimoto, Y.; Akimitsu, K.; Ohtani, K.; Kodama, M.; Akagi, Y.; Egusa, M.; Yamamoto, M.; Otani, H.; *FEMS Microbiol. Rev.* **2013**, *37*, 44. [Crossref]

30. Hu, Z.; Chang, X.; Dai, T.; Li, L.; Liu, P.; Wang, G.; Liu, P.; Huang, Z.; Liu, X.; *Evol. Bioinform. Online* **2019**, *15*, 1176934319838518. [Crossref]

31. Fürstenberg-Hägg, J.; Zagrobelny, M.; Bak, S.; *Int. J. Mol. Sci.* **2013**, *14*, 10242. [Crossref]

32. Howe, G. A.; Jander, G.; *Annu. Rev. Plant Biol.* **2008**, *59*, 41. [Crossref]

33. Petterson, D. S.; Harris, D. J.; Allen, D. G. In *Toxic Substances in Crop Plants*; D'Mello, J. P. F.; Duffus, C. M.; Duffus, J. H.,

eds.; The Royal Society of Chemistry: Cambridge, England, 1991, p. 148.

34. Harborne, J. B.; *Introduction to Ecological Biochemistry*, 3rd ed.; Academic Press: London, England, 1988.

35. Sharma, P.; Kothari, S. L.; Rathore, M. S.; Gour, V. S.; *Turk. J. Bot.* **2018**, *42*, 135. [Crossref]

36. Maxwell, D. J.; Partridge, J. D.; Roberts, N. W.; Boonham, N. W.; Foster, G. D.; *PLoS One* **2016**, *11*, 1209. [Crossref]

37. Farag, M. A.; Otify, A.; Porzel, A.; Michel, C. G.; Elsayed, A.; Wessjohann, L. A.; *Anal. Bioanal. Chem.* **2016**, *408*, 3125. [Crossref]

38. Leal, A. E. B. P.; Oliveira, A. P.; Santos, R. F.; Soares, J. M. D.; Lavor, E. M.; Pontes, M. C.; Lima, J. C.; Santos, A. D. C. S.; Tomaz, J. C.; Oliveira, G. G.; Carnevale Neto, F.; Lopes, N. P.; Rolim, L. A.; Almeida, J. R. G.; *Nat. Prod. Res.* **2020**, *34*, 995. [Crossref]

39. Nicholson, R. L.; Hammerschmidt, R.; *Annu. Rev. Phytopathol.* **1992**, *30*, 369. [Crossref]

40. Etalo, D. W.; Stulemeijer, I. J. E.; Van Esse, H. P.; De Vos, R. C. H.; Bouwmeester, H. J.; Joosten, M. H. A. J.; *Plant Physiol.* **2013**, *162*, 1599. [Crossref]

41. Asselin, J. E.; Lin, J.; Perez-Quintero, A. L.; Gentzel, I.; Majerczak, D.; Opiyo, S. O.; Zhao, W.; Paek, S. M.; Kim, M. G.; Coplin, D. L.; Blakeslee, J. J.; Mackey, D.; *Plant Physiol.* **2015**, *167*, 1117. [Crossref]

42. Zhou, H.; Lin, J.; Johnson, A.; Morgan, R. L.; Zhong, W.; Ma, W.; *Cell Host Microbe* **2011**, *9*, 177. [Crossref]

43. Castro-Moretti, F. R.; Gentzel, I. N.; Mackey, D.; Alonso, A. P.; *Metabolites* **2020**, *10*, 52. [Crossref]

44. Kuhn, C. W.; *Phytopathology* **1964**, *54*, 739.

45. Cerqueira-Silva, C. B. M.; Moreira, C. N.; Figueira, A. R.; Corrêa, R. X.; Oliveira, A. C.; *Genet. Mol. Res.* **2008**, *7*, 1209. [Crossref]

46. Abreu, E. F. M.; Tinoco, M. L. P.; Andrade, E. C.; Aragão, F. J. L.; *Genet. Mol. Res.* **2012**, *11*, 3146. [Crossref]

47. XCMS online, https://xcmsonline.scripps.edu/, accessed in May 2022.

48. MetaboAnalyst 3.0, http://www.metaboanalyst.ca/, accessed in May 2022.

49. Johansen, D. A.; *Plant Microtechnique*; McGraw Hill: London, England, 1940.

50. Kraus, J. E.; Arduin, M.; *Manual Básico de Métodos em Morfologia Vegetal*, 1st ed.; EDUR: Rio de Janeiro, Brazil, 1997.

51. O'Brien, T. P.; Feder, N.; Mccully, M. E.; *Protoplasma* **1964**, *59*, 368.

52. *AxioVision Rel. 4.8.2 Software*; Carl Zeiss MicroImaging GmbH, Germany, 2016.

53. Aguiar, T. V.; Santos, B. F. S.; Azevedo, A. A.; Ferreira, R. S.; *Planta Daninha* **2007**, *25*, 649. [Crossref]

54. *R Foundation for Statistical Computing*; R Core Team, Viena, Austria, 2013.

55. Wang, Y.; Harrington, P. B.; Chen, P.; *Anal. Bioanal. Chem.* **2020**, *412*, 7669. [Crossref]

56. Liu, Y.; Xue, A.; Ding, L.; Hao, Y.; Liu, H.; Cui, M.; Liu, L.; Nie, Z.; Luo, L.; *Anal. Bioanal. Chem.* **2020**, *412*, 3091. [Crossref]

57. Matos, T. K. B.; Guedes, J. A. C.; Alves Filho, E. G.; Luz, L. R.; Lopes, G. S.; Nascimento, R. F.; Sousa, J. A.; Canuto, K. M.; Brito, E. S.; Dias-Pini, N. S.; Zocolo, G. J.; *J. Braz. Chem. Soc.* **2021**, *32*, 1617. [Crossref]

58. Melo, G. M. A.; Silva, M. C. R.; Guimarães, T. P.; Pinheiro, K. M.; Matta, C. B. B.; Queiroz, A. C. Q.; Pivatto, M.; Bolzani, V. S.; Alexandre-Moreira, M. S.; Viegas Jr., C.; *Phytomedicine* **2014**, *21*, 277. [Crossref]

59. Pivatto, M.; Baccini, L. R.; Sharma, A.; Nakabashi, M.; Danuello, A.; Viegas Jr., C.; Garcia, C. R. S.; Bolzani, V. S.; *J. Braz. Chem. Soc.* **2014**, *25*, 1900. [Crossref]

60. Viegas Jr., C.; Bolzani, V. S.; Pimentel, L. S. B.; Castro, N. G.; Cabral, R. F.; Costa, R. S.; Floyd, C.; Rocha, M. S.; Young, M. C. M.; Barreiro, E. J.; Fraga, C. A. M.; *Bioorg. Med. Chem.* **2005**, *13*, 4184. [Crossref]

61. Bravo, J. A.; Lavaud, C.; Bourdy, G.; Deharo, E.; Gimenez, A.; Michel, S.; *Rev. Bol. Quim.* **2002**, *19*, 12. [Link] accessed in May 2022

62. Thomazzi, S. M.; Silva, C. B.; Silveira, D. C.; Vasconcellos, C. L.; Lira, A. F.; Cambui, E. V.; Estevam, C. S.; Antoniolli, A. R.; *J. Ethnopharmacol.* **2010**, *127*, 451. [Crossref]

63. Zaheer-ul, H.; Wellenzohn, B.; Tonmunphean, S.; Khalid, A.; Choudhary, M. I.; Rode, B. M.; *Bioorg. Med. Chem. Lett.* **2003**, *13*, 4375. [Crossref]

64. Choudhary, M. I.; Nawaz, S. A.; Zaheer-Ul-Haq; Azim, M. K.; Ghayur, M. N.; Lodhi, M. A.; Jalil, S.; Khalid, A.; Ahmed, A.; Rode, B. M.; Atta-Ur-Rahman; Gilani, A. U.; Ahmad, V. U.; *Biochem. Biophys. Res. Commun.* **2005**, *332*, 1171. [Crossref]

65. Ogungbe, I. V.; Ng, J. D.; Setzer, W. N.; *Future Med. Chem.* **2013**, *5*, 1777. [Crossref]

66. Gomez, A. A.; Baptista, Z. P. T.; Mandova, T.; Barouti, A.; Kritsanida, M.; Grougnet, R.; Vattuone, M. A.; Sampietro, D. A.; *Nat. Prod. Res.* **2020**, *34*, 3299. [Crossref]

67. Xue, F.; Seto, C. T.; *Bioorg. Med. Chem.* **2020**, *14*, 8467. [Crossref]

68. Paprocka, M.; Gliszczyńska, A.; Dancewicz, K.; Gabryś, B.; *Molecules* **2018**, *23*, 2362. [Crossref]

69. Zobnina, V.; Lambreva, M. D.; Rea, G.; Campi, G.; Antonacci, A.; Scognamiglio, V.; Giardi, M. T.; Polticelli, F.; *Photosynth. Res.* **2017**, *131*, 15. [Crossref]

70. Zhao, J.; Liu, Q.; Zhang, H.; Jia, Q.; Hong, Y.; Liu, Y.; *Plant Physiol.* **2013**, *161*, 374. [Crossref]

71. Maciejewska, U.; Polkowska-Kowalczyk, L.; Swiezewska, E.; Szkopinska, A.; *Acta Biochim. Pol.* **2002**, *49*, 775.

72. Liu, M.; Lu, S.; *Front. Plant Sci.* **2016**, *7*, 1898. [Crossref]

73. Laurençon, L.; Sarrazin, E.; Chevalier, M.; Prêcheur, I.; Herbette, G.; Fernandez, X.; *Phytochemistry* **2013**, *86*, 103. [Crossref]

74. Matušinský, P.; Zouhar, M.; Pavela, R.; Nový, P.; *Ind. Crops Prod.* **2018**, *67*, 208. [Crossref]

75. Singh, B.; Kaur, A.; *LWT* **2018**, *87*, 93. [Crossref]

76. Zhao, Y. L.; Cai, G. M.; Hong, X.; Shan, L. M.; Xiao, X. H.; *Phytomedicine* **2008**, *15*, 253. [Crossref]

77. Huang, H. C.; Liao, S. C.; Chang, F. R.; Kuo, Y. H.; Wu, Y. C.; *J. Agric. Food Chem.* **2003**, *51*, 4916. [Crossref]

78. Waller, G. R.; Jurzysta, M.; Thorne, R. L. Z.; *Bot. Bull. Acad. Sin.* **1993**, *34*, 1. [Link] accessed in May 2022

79. Zhang, J.; Zhang, Z.; Chukkapalli, V.; Nchoutmboube, J. A.; Li, J.; Randall, G.; Belov, G. A.; Wang, X.; *Proc. Natl. Acad. Sci.* **2016**, *113*, e1064. [Crossref]

80. Reid, T.; Kashangura, C.; Chidewe, C.; Benhura, M. A.; Stray-Pedersen, B.; Mduluza, T.; *Int. J. Med. Mushrooms* **2019**, *21*, 713. [Crossref]

81. Li, S. S.; Liu, Y.; Li, H.; Wang, L. P.; Xue, L. F.; Yin, G. S.; Wu, X. S.; *Eur. Rev. Med. Pharmacol. Sci.* **2019**, *23*, 3940. [Crossref]

82. Abdullah, M.; Kornegay, J. N.; Honcoop, A.; Parry, T. L.; Balog-Alvarez, C. J.; O'Neal, S. K.; Bain, J. R.; Muehlbauer, M. J.; Newgard, C. B.; Patterson, C.; Willis, M. S.; *Metabolites* **2017**, *7*, 38. [Crossref]

83. Barbosa, N. C. S.: *Anatomia Foliar e Diversidade Genética em Passiflora spp. (Passifloraceae L.) Resistentes ao Cowpea Aphid-Borne Mosaic Virus (CABMV)*; MSc Dissertation, Universidade Federal da Bahia, Salvador, Brazil, 2016. [Crossref]

84. Thompson, K. F.; *Nature* **1963**, *198*, 209. [Link] accessed in May 2022

85. Costa, E. M. R.; Marchese, A.; Maluf, W. R.; Silva, A. A.; *Rev. Ciênc. Agron.* **2014**, *45*, 146. [Crossref]

86. Tsumuki, H.; Kanehisa, K.; Kawada, K.; *Appl. Entomol. Zool.* **1989**, *4*, 295.

87. Shepherd, T.; Robertson, G. W.; Griffiths, D. W.; Birch, A. N. E.; *Phytochemistry* **1999**, *52*, 1255. [Crossref]

88. White, C.; Eigenbrode, S. D.; *Environ. Entomol.* **2000**, *29*, 773. [Crossref]

89. Khan, M. A. U.; Shahid, A. A.; Rao, A. Q.; Shahid, N.; Latif, A.; Din, S.; Husnain, T.; *Adv. Life Sci.* **2015**, *2*, 58. [Link] accessed in May 2022

90. Scatena, V. L.; Segecin, S.; *Rev. Bras. Bot.* **2005**, *28*, 635. [Crossref]

91. Lima Jr., E. C. L.; Alvarenga, A. A.; Castro, E. M.; Vieira, C. V.; Barbosa, J. P. R. A. D.; *Rev. Arvore* **2006**, *30*, 33. [Crossref]

92. Gonçalves, Z. S.; Jesus, O. N.; Lima, L. K. S.; Corrêa, R. X.; *Arch. Virol.* **2021**, *166*, 2419. [Crossref]

93. Santos, E. A.; Viana, A. P.; Freitas, J. C. O.; Silva, F. H. L.; Rodrigues, R.; Eiras, M.; *Eur. J. Plant Pathol.* **2015**, *143*, 85. [Crossref]